Raman spectroscopic study of the pressure-induced coordination change in GeO_2 glass

Dan J. Durben and George H. Wolf
Department of Chemistry, Arizona State University, Tempe, Arizona 85287
(Received 16 July 1990)

Raman spectra of GeO_2 glass are recorded *in situ* as a function of pressure to 56 GPa at room temperature. Under initial compression to 6 GPa the main 419-cm^{-1} Raman band shifts to higher frequency and broadens with a gradual loss of intensity. These spectral changes are consistent with an increase in distortion of GeO_4 tetrahedra and a decrease in the intertetrahedral bond angle with pressure. Between 6 and 13 GPa (the pressure range of the reported fourfold- to sixfold-coordination change of Ge in germania glass) the main Raman band broadens, and the scattering intensity is dramatically reduced with little shift in peak frequency. This pressure interval is also marked with the appearance and growth of a broad low-frequency band near 240 cm^{-1}. The inferred pressure-induced coordination change occurs without the formation of nonbridging oxygens. Above 13 GPa no further major structural changes are indicated by the Raman data taken with pressures up to 56 GPa. On decompression the back transformation of octahedral Ge to tetrahedral coordination is complete but exhibits a large hysteresis. The Raman data indicate that the high-coordinate germanium species are retained down to pressures of at least 2.3 GPa. In samples decompressed from high pressures, the intensity of the 520-cm^{-1} "defect" band is considerably enhanced relative to that in normal germania glass, consistent with an increase in three-membered-ring population. It is proposed that a large component of this increase in three-membered rings is a result of the reversion of ^{III}O species to tetrahedra-bridging ^{II}O species under decompression.

I. INTRODUCTION

The relationship between the structural and physical properties of the technologically and geologically important tetrahedral oxides has been the subject of much fundamental interest. Structural models based on an open three-dimensional network of corner-shared tetrahedra have been used to explain many of the unusual and interesting physical properties of the liquid and amorphous states of these systems. Anomalous waterlike behavior, such as the density maximum with temperature in the supercooled liquid and glass states of silica,[1] has been explained through the competition between the high energetic stability and the low configurational entropy of the open tetrahedral framework.

Disruption of the tetrahedral framework has a profound effect on the physical properties of these network liquids and glasses. Under chemical substitution, such as addition of alkali or alkaline-earth oxides to silica, the tetrahedral framework can be broken by replacement of network linkages with less directional bonds, resulting in an increase in configurational entropy[2] and a corresponding reduction in the liquid-state viscosity.[3] Destabilization of the tetrahedral network can also occur through coordination changes of network cations as observed upon addition of alkali oxides to germania.[4–10]

The effect of pressure on the tetrahedral framework structure of amorphous silicates and germanates is analogous to that of chemical substitution. Pressure-induced disruption of the tetrahedral network structure, either through modifications of the medium-range order or through coordination changes, is manifested in the anomalous physical properties of many silicates and germanates. These include the increase in compressibility[11,12] and thermal expansivity[13] of silica glass with pressure, the decrease in the liquid-state viscosity of silica and germania with increasing pressure,[14–16] and the irreversible densification of their glasses upon pressure cycling.[12,14,17–21]

While coordination changes of network cations may be a significant mechanism of pressure-induced tetrahedral network destabilization in MO_2-type oxides, direct *in situ* verification of pressure-induced coordination changes has been difficult to confirm in these liquids and glasses. This is in contrast to the well-characterized tetrahedral to octahedral coordination transformations observed in the crystalline analogs of these materials at high pressures.[22] Coordination changes have also been proposed as the underlying mechanism of the solid-state amorphization of several tetrahedral based crystals under extreme superpressing.[23] It is thus plausible that similar coordination changes occur in the liquid and amorphous phases of MO_2-type oxides at high pressures.

Vibrational spectroscopy, although an indirect structural probe, has provided some of the only *in situ* data on the structural properties of MO_2-type oxide glasses as a function of pressure. Reversible changes in the infrared absorption spectra of SiO_2 glass above 20 GPa have been interpreted to indicate a silicon coordination change.[23] The Raman spectra of silica and alkalisilicate glasses display similar trends at high pressure that may be consistent with a silicon coordination change in silicate glasses above 30 GPa.[24,25] However, the lack of experimental data and theoretical calculations on high-

pressure crystal and amorphous phases of MO_2-type oxides precludes assignment of the Raman bands in terms of structural features.

Amorphous germanium dioxide (g-GeO_2) is an especially useful model for investigating pressure-induced structural changes in tetrahedral oxide glasses and melts.[26] Germania is isotypic with silica and exhibits similar pressure dependences of physical properties.[14,18,20,21] Pressure-induced structural changes in germania are believed to be similar to those that occur in silica under pressure, but are expected to occur at considerably lower pressures.[27] This is evidenced by the thermodynamic stability of both the IV-coordinate α-quartz and VI-coordinate rutile forms of crystalline GeO_2 at ambient pressure,[28,29] whereas SiO_2 is thermodynamically stable only in IV-coordinate polymorphs at ambient pressure.

Recently, the first direct evidence of a pressure-induced coordination change in a tetrahedral oxide was reported in an *in situ* x-ray-absorption study of g-GeO_2 at room temperature in a diamond anvil cell.[30] The x-ray data indicated an increase in the Ge—O bond length consistent with a fourfold- to sixfold-Ge-coordination change under compression at pressures between 6.6 and 12 GPa. Two distinct Ge coordination sites were indicated in the transition region rather than a progressive evolution of the coordination number of a Ge site. Under decompression the coordination transition displayed a large hysteresis before complete reversion back to tetrahedrally coordinated Ge below 2 GPa.

The present study utilizes Raman spectroscopy to study the deformation mechanisms and vibrational properties of germania glass *in situ* at 298 K to pressures up to 56 GPa in a diamond anvil cell. The recently reported extended x-ray-absorption fine-structure (EXAFS) study of g-GeO_2 (Ref. 30) provides an excellent calibration for the interpretation of the high-pressure Raman data of g-GeO_2 and analogous MO_2-type systems.

II. EXPERIMENT

Germanium dioxide glass was prepared from electronic-grade powdered hexagonal GeO_2 (Penn Rare Metals Div.) by heating in air at 1400 °C for 30 min in a platinum crucible, followed by air quenching to room temperature. High-pressure experiments were performed at 298 K in a gasketed piston-cylinder-type diamond anvil cell[31,32] employing low-fluorescence type-I diamonds. The gasket was formed from a 250-μm-thick rhenium foil, first preindented, then laser drilled to create a sample chamber approximately 200 μm in diameter and 50 μm deep. Several small (< 10 μm) ruby chips, used as a pressure indicator, were scattered across the culet face of one of the diamonds. Pressure was determined by the calibrated pressure shift in the ruby R_1 fluorescence line.[33]

Reported Raman spectra are from GeO_2 glass samples loaded directly into the sample chamber without a pressure-transmitting medium. Standard alcohol pressure-transmitting solvents were avoided as g-GeO_2 has been reported to react under pressure with a methanol-ethanol mixture.[34] Reported spectral changes were reproduced using argon as a pressure-transmitting medium, although the low-frequency area of the weak g-GeO_2 Raman signal was obscured at elevated pressures by an increase in the low-frequency scattering of the pressure medium.

Raman scattering was excited in the sample by the 488-nm line of a Coherent (90-5) Ar^+ ion laser. The laser beam was focused to a 30 μm spot on the sample. The Raman signal was collected using a 135° scattering geometry through a long working distance 50X Mitutoyo microscope objective in a modified Olympus (BH-2) petrographic microscope. A spatial filter, placed at an intermediate image plane in the collection optics, was used to reduce contamination of the Raman signal from diamond fluorescence. The Raman scattering data were collected with an Instruments S.A. triple spectrometer (S3000) coupled with both a Princeton Instruments intensified diode array detector (IY-750) for multichannel detection and a photomultiplier tube for scanning mode detection. The spectrometer entrance slit was set at 100 μm giving a spectral resolution of approximately 10 cm^{-1}. A polarization analyzer was used at the entrance of the spectrometer, and all reported spectra were obtained in a HH scattering geometry.

III. RESULTS AND DISCUSSION

A. Ambient structure of GeO_2 glass

The ambient structure of normal GeO_2 glass has been investigated with a variety of experimental techniques including x-ray diffraction,[35–37] neutron diffraction,[38–41] EXAFS,[7,42,43] and vibrational spectroscopy.[14,28,44–48] The structural short-range order of g-GeO_2 closely resembles the α-quartz configuration of crystalline GeO_2. Each germanium is bonded to four oxygen atoms in a tetrahedral framework arrangement, with each oxygen coordinated to two germaniums, similar to the tetrahedral arrangement in g-SiO_2. Reported nearest-neighbor atomic distances vary with measurement technique but are in general agreement with the mean Ge—O bond distance of 1.739 Å, Ge-Ge nearest distance of 3.185 Å, and O-O nearest distance of 2.836 Å given by Desa and Wright.[40] The GeO_4 tetrahedra in germania glass are more distorted than the analogous SiO_4 tetrahedra in silica glass. The longer Ge—O bond length, relative to the much shorter 1.62-Å Si—O bond length,[49] produces less steric crowding of oxygens around the central cation. Distortion in the GeO_4 tetrahedra is manifested by a large variation (104°–115°) and bimodal distribution in the O—Ge—O dihedral bond angle, rather than a variation in Ge—O bond length.[40,50] In comparison, the dihedral bond angle of SiO_4 tetrahedra in silica glass is more tightly constrained (108°–111°).[50]

The medium-range order of g-GeO_2 is commonly described as an open three-dimensional tetrahedral framework. The most widely accepted theoretical model used to describe the nature of this framework is the continuous random network (CRN) of corner-shared tetrahedra as first proposed by Zachariasen[51] for MO_2-type glasses. Disorder is introduced into the glass by a continuous distribution of Ge—O—Ge intertetrahedral angles and tor-

tional angles, i.e., relative rotations of neighboring tetrahedra. The average Ge—O—Ge intertetrahedral angle of 133° (Refs. 35, 40, and 48) is tighter with a narrower distribution (approximately 10°) (Refs. 36 and 42) compared with the average 144° and 120°–180° intertetrahedral-angle distribution found in g-SiO_2.[49] Cation-cation nonbonded repulsions have been invoked to account for the intertetrahedral-angle differences in MO_2-type compounds.[52–54] The longer Ge—O bond length, relative to the Si—O bond length, allows for a tighter intertetrahedral angle in g-GeO_2 before nonbonded cation contact.

An alternative to the CRN model for describing tetrahedral oxide glass structure is the cluster, or microcrystalline model.[55–59] In this model the glass is built from an array of microcrystals. Disorder is introduced by broken chemical bond order at cluster edges, suggesting a large density of dangling or reconstructed bonds on internal surfaces of the clusters. Others have suggested models for the structure of g-GeO_2 intermediate between the CRN and microcrystalline extremes.[9,10,37,41]

A feature of both the CRN and microcrystalline models is the probability of closed rings of atoms in the structures of g-GeO_2 and g-SiO_2.[40,58,60–62] However, a difference in the ring statistics of g-GeO_2 and g-SiO_2 is expected. This is a reflection of the tighter distribution of intertetrahedral angles in g-GeO_2 which precludes the degree of ring irregularity found in g-SiO_2. In the CRN model, the g-GeO_2 network is dominated by rings composed of six germaniums bridged by oxygens (six-membered rings).[48,63] A relatively large population of three-membered rings is probable due to the favorable 130.5° angle of this ring structure compared with the average g-GeO_2 intertetrahedral angle of 133°.[60,62] In contrast to the planar three-membered rings predicted for g-SiO_2,[60–63] many of the GeO_2 three-membered rings may be nonplanar based on molecular cluster calculations[62] and a preliminary g-GeO_2 random network model.[40] In the microcrystalline model, six-membered rings dominate in both the g-GeO_2 and g-SiO_2 networks, but the small ring formation found in the CRN model is discounted.[58]

B. Ambient Raman spectrum of GeO_2 glass

Interpretations of the Raman bands of GeO_2 glass have progressively developed by exploiting a variety of experimental techniques including isotopic substitution,[47] neutron bombardment,[45] alkali substitution,[4,5,64,65] SiO_2 substitution,[48,66] and OH substitution.[21,67] Vibrational dynamics calculations based on the CRN model have also aided the correlation between structural vibrations and Raman active modes.[47,68–76] Comparisons with the much studied ambient g-SiO_2 Raman spectrum[44,46,60,61,75,77] have also been important in the interpretation of the g-GeO_2 Raman spectrum. Many features of the two spectra are analogous, reflecting the similarity of the structures of g-GeO_2 and g-SiO_2. Differences in the frequency shift and bandwidth of equivalent modes are largely a consequence of the mass difference between Ge and Si and the tighter configurational constraints in the GeO_2 glass network.[48]

The ambient Raman spectrum of GeO_2 glass is shown in Fig. 1. The dominant feature in the Raman spectrum is a strong, polarized band centered at 419 cm^{-1}. This band has been assigned to the symmetric stretching (SS) of bridging oxygens in a line bisecting the Ge—O—Ge plane[14,75] in predominantly six-membered rings,[21,48] equivalent to the strong 437-cm^{-1} band of g-SiO_2.[14,48] The 419-cm^{-1} band of g-GeO_2 has a much sharper bandwidth than the 437-cm^{-1} band of g-SiO_2, indicative of the tighter distribution of intertetrahedral angles in g-GeO_2.

The broad high-frequency shoulder of the main Raman band contains a feature near 520 cm^{-1}. The intensity of this band is enhanced in neutron irradiated samples[45] and is thought to be analogous to the same structural unit represented by the 606-cm^{-1} "defect" band in g-SiO_2.[45,46] However, the structural origin of the 520-cm^{-1} band is still debated. One interpretation assigns this band to broken-bond or other-bond defects in the network,[21,45,48] although Ge-Ge and O-O defects are unlikely.[45] Phillips[58] suggests the 520-cm^{-1} band is a ring mode in the microcystalline model, arising from a rearrangement of cluster surfaces which could create rings of unspecified size by intercluster cross linking. Galeener and co-workers[47,60] assign this band to three-membered rings embedded in a CRN, consistent with both the sharpness of the deconvoluted 520-cm^{-1} band and the pure oxygen breathing motion of a highly symmetric unit inferred by its isotope shift. Regardless of the exact origin, the intensity of the 520-cm^{-1} band may be used as a reflection of the amount of Raman active defects in g-GeO_2.

Two other bands have been resolved from the high-

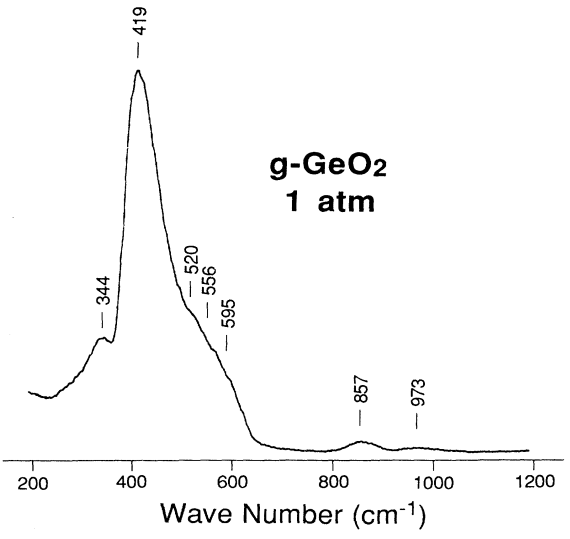

FIG. 1. HH Raman spectrum of GeO_2 glass taken at ambient conditions.

frequency shoulder of the main Raman band of g-GeO_2 at about 566 and 595 cm^{-1}. These bands have been respectively assigned to transverse optical (TO) and longitudinal optical (LO) vibrational modes involving significant motion of both Ge and O.[44,47] These bands are the mass-shifted equivalent to the TO-LO pair in the 800-cm^{-1} mode of g-SiO_2.

Other features of the ambient Raman spectrum of g-GeO_2 include two weak depolarized high-frequency bands at 857 and 973 cm^{-1}. These have been respectively assigned to the TO and LO asymmetric stretching (AS) modes of bridging oxygens, analogous to the 1060- and 1190-cm^{-1} bands in g-SiO_2.[44,48] A low-frequency feature near 344 cm^{-1}, observed in the Raman spectrum of g-GeO_2, has no analogous band in g-SiO_2. From isotopic substitution studies, the mode associated with this band has predominantly Ge motion with very little O motion,[47] but its specific structural origin is still unknown.

Significantly missing from the g-GeO_2 spectrum are any of the strong, polarized, high-frequency nonbridging oxygen SS bands observed near 800–900 cm^{-1} in alkali germanates,[4,5,64,65] inferring the absence of nonbridging oxygens in the structure of normal g-GeO_2.[5,14,78]

C. Compression of GeO_2 glass

Figure 2 shows the *in situ* Raman spectra of GeO_2 glass as a function of pressure to approximately 13 GPa, taken at ambient temperature under increasing compression. With initial compression up to 5.6 GPa the main 419-cm^{-1} Raman band rapidly shifts to higher frequency, broadens, and gradually loses intensity. There is no significant intensity change in the 520-cm^{-1} defect band. The high-frequency 857- and 973-cm^{-1} bands show a slight negative frequency shift, and the low-frequency 344-cm^{-1} band is retained with a slight positive frequency shift. These observations are consistent with earlier *in situ* high-pressure g-GeO_2 Raman data,[34] except that no large increase in the Rayleigh tail, attributed to increasing disorder in the glass, was observed. Raman frequency shifts in this low-pressure region are also qualitatively similar to those observed in samples of g-GeO_2 that have been densified by neutron irradiation.[45]

A compression mechanism for g-GeO_2 in the pressure range from 1 atm to 5.6 GPa, consistent with the observed Raman data and also consistent with *in situ* EXAFS,[30] and neutron and x-ray diffraction studies of g-GeO_2 and α-quartz GeO_2 under compression,[37,41,50,79] is one dominated by a continuous increase in tetrahedral distortion accompanied by a small decrease in the intertetrahedral Ge—O—Ge bond angle. In this model, increasing compression distorts the GeO_4 tetrahedra by further increasing the bimodal distribution of the O—Ge—O dihedral angles.

The gradual intensity loss of the main SS Raman band is consistent with tetrahedral distortion. The main Raman band in g-GeO_2 occurs at a minimum in the neutron vibrational density of states.[80] The SS mode, belonging to the totally symmetric representation of the local point-group symmetry, is thus associated with a few vibrational modes that have a relatively large Raman cross section. The intensity of the main Raman band would thus be sensitive to the disruption of symmetry around the bridging oxygens caused by the pressure-induced decrease in short-range order.

While tetrahedral distortion may be the dominant mechanism for g-GeO_2 in this pressure regime, there is also a measurable decrease in the Ge-Ge nearest-neighbor distance.[50] This decrease further constrains the magnitude and distribution of Ge—O—Ge intertetrahedral angles, resulting in some increase in medium-range order. This observation is consistent with the positive frequency shift of the main Raman band and negative frequency shift of the high-frequency bands in g-GeO_2 as seen in g-SiO_2.[24,75]

There are some important differences in the low-pressure deformation mechanisms of g-GeO_2 and that indicated for g-SiO_2.[19,20,24,26,81] In g-SiO_2 the intial (<8

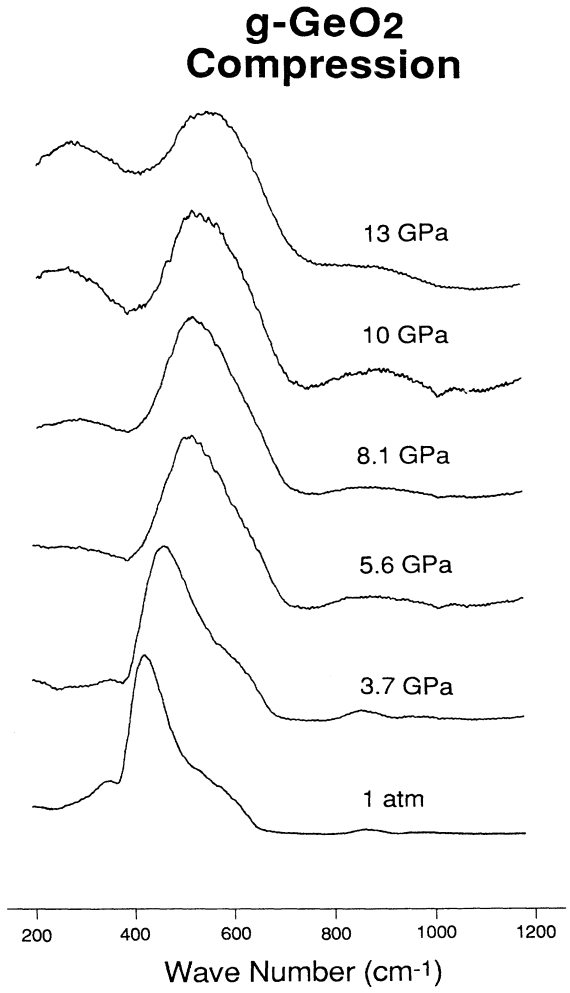

FIG. 2. *In situ HH* Raman spectra of GeO_2 glass as a function of pressure under increasing compression to 13 GPa.

GPa) compression mechanism is thought to be dominated by a decrease in the average value and variation of intertetrahedral angle distribution with negligible tetrahedral distortion. Thus, initial compression in g-SiO_2 could be accommodated by tightening the average intertetrahedral angle to a value approaching the ambient g-GeO_2 intertetrahedral angle. This collapse of the open ring structure is reflected by the decrease in bandwidth of the main Raman band of g-SiO_2 under compression up to 8 GPa.[24]

Tetrahedral distortion becomes an important deformation mechanism in g-SiO_2 only at a pressure high enough to have rotated the tetrahedra to positions creating strained cation-cation repulsions as is nearly the case with ambient g-GeO_2. Indeed, the Raman spectrum of g-SiO_2 at 8 GPa (Ref. 24) qualitatively resembles the ambient spectrum of g-GeO_2. With increasing compression above 8 GPa up to approximately 30 GPa, the Raman spectra of g-SiO_2 follow a pattern similar to compression of g-GeO_2 up to 5.6 GPa. By analogy with the g-GeO_2 Raman spectra this may indicate increasing tetrahedral distortion in g-SiO_2 above 8 GPa. The higher pressures may reflect the difficulty in distorting the more rigid SiO_4 tetrahedra compared to the more easily distorted GeO_4 tetrahedra.

A change in the compression mechanism in g-GeO_2 is suggested by the Raman data above 5.6 GPa. Between 5.6 and 13 GPa the main Raman band broadens with little shift in peak frequency. In addition, while not evident in the scaled spectra of Fig. 2, the main Raman band undergoes a marked, near tenfold decrease in intensity over this pressure range, falling to approximately the same height as its high-frequency shoulder. In this pressure range, the high-frequency 857- and 973-cm^{-1} bands coalesce and the 344-cm^{-1} band disappears. This pressure regime is also marked by the appearance of a low-frequency band not observed in previous high-pressure Raman studies of g-GeO_2. This broadband first appears at approximately 240 cm^{-1} and builds in intensity with increasing pressure to 13 GPa. At 13 GPa the Raman spectrum of g-GeO_2 is characterized by three broad but distinct bands at approximately 275, 550, and 890 cm^{-1}.

The pressure range of 5.6–13 GPa also matches the transition region of the transformation from fourfold to sixfold Ge coordination observed in the *in situ* EXAFS study of g-GeO_2 by Itie *et al.*[30] Thus the changes in the Raman spectrum can be expected to reflect the transformation from corner-shared tetrahedra to edge-shared octahedra. The observed changes in the g-GeO_2 Raman spectrum are in disagreement with previous predictions that a coordination change would cause dramatic alterations in the Raman spectrum,[14,78] including an expected appearance of a high-frequency band near 700 cm^{-1} analogous to that found in the rutile GeO_2 Raman spectrum.[14] Instead, the coordination change in g-GeO_2 is marked by a change in the pressure derivative of the frequency shift of the main Raman band, a strong broadening and weakening of this band, and the appearance of a low-frequency band near 240 cm^{-1}.

Some similarities are observed in the behavior of the Raman spectrum of g-SiO_2, but at much higher pressures.[24] Above 30 GPa the main Raman band stops shifting with pressure and dramatically loses intensity, becoming undetectable above 40 GPa. A gradual coordination change in g-SiO_2 near this same general pressure range has been inferred from *in situ* infrared spectra.[23] Comparisons with the g-GeO_2 Raman spectra seem to substantiate the spectroscopic evidence of a gradual coordination change in g-SiO_2 at very high pressures.

Transformation of tetrahedrally coordinated germanium or silicon atoms to higher coordination states in the fully polymerized glasses requires the involvement of bridging oxygens, forming three-coordinate oxygen (^{III}O) species. Proposed mechanisms for pressure-induced coordination changes in MO_2-type glasses have typically required a breakdown of the network structure leading to the formation of nonbridging oxygens as a prerequisite to coordination changes.[14,78] However, the deformation mechanism in g-GeO_2 from 5.6 to 13 GPa does not appear to involve the formation of nonbridging oxygens. This is evident by the lack of enhancement of Raman bands in the high-frequency region as observed in alkali substituted germanates.[4,5,64,65] Rather, it appears the gradual pressure-induced transformation of bridging ^{II}O species to the higher-coordinate ^{III}O species occurs without bond breaking.

Figure 3 shows the composite Raman spectra of g-GeO_2 under increasing compression to approximately 56 GPa. No further dramatic changes in the structure of the glass between 13 and 56 GPa are inferred from the spectra. There is a very gradual broadening and positive frequency shift of the remaining three bands to approximately 350, 645, and 910 cm^{-1} at 56 GPa. However, these bands do persist to very high pressures, as opposed to the Raman bands of g-SiO_2 which become indistinct above 40 GPa.[24]

Because of the reduced stray-light rejection in multichannel detection, the Raman signal was strongly contaminated by stray Rayleigh scattered light below 100 cm^{-1}. To examine the low-frequency region of g-GeO_2 at high pressures more closely, spectra were obtained in a single-channel scanning mode. Figure 4 shows scanning data of g-GeO_2 taken at 32 GPa between 10 and 1250 cm^{-1}. At this pressure all the germaniums can be expected to be sixfold coordinated and all the oxygens threefold coordinated.[30] This high-pressure Raman spectrum contains the boson peak characteristic of glasses, and Raman active modes near 330, 610, and 890 cm^{-1} as also observed in the multichannel spectra.

Some preliminary observations related to the origin of the low-frequency Raman band of GeO_2 glass at high pressures can be presented. Bands at 205 and 285 cm^{-1} are observed in Ge-rich GeO_2 glass.[45] Originally interpreted as Ge—Ge bond vibrations, the ^{III}O species would also be expected in Ge-rich glass. Also containing a low-frequency mode is the ambient Raman spectrum of rutile GeO_2, with a B_{1g} mode at 166 cm^{-1}.[5,14,28] From lattice-dynamical calculations this mode is associated with octahedral librations.[82] A low-frequency band is also observed in the Raman spectrum of some highly substituted alkali germanate glasses.[4,5,64,65] Significantly, no low-

frequency band is observed in either high-pressure or alkali-substituted silica glass.

D. Decompression of GeO_2 glass

Most experimental information concerning the high-pressure structural properties of silicate and germanate glasses and liquids has been inferred from ambient pressure data on samples quenched from high pressure. Therefore it is of great interest to know the degree of reversibility of pressure-induced structural changes.

Figure 5 shows the Raman spectra of GeO_2 glass upon decompression. The spectral changes strongly parallel the EXAFS decompression results of Itie *et al.*[30] The high-pressure spectral features exhibit a large hysteresis and are retained to at least 2.3 GPa. Below 2.3 GPa, the spectrum dramatically snaps back to a form showing all the general features of the original ambient spectrum. The low-frequency band disappears, the 344-cm^{-1} band reappears, and the broad high-frequency band splits back into separate TO and LO modes. The most dramatic change, while not as evident in the scaled spectra, is the large, sudden increase in intensity of the main Raman band and its high-frequency shoulder. This implies that the vibrational origin of these modes may be different at low and high pressure. It is clear from the spectra that the high-pressure structure is not quenched to ambient pressure.

The strong enhancement of the 520-cm^{-1} defect band as g-GeO_2 is decompressed below 2.3 GPa implies an increase in defect population. Significantly, this strong enhancement is observed only upon decompression. The enhancement of the 520-cm^{-1} defect band on decompression is consistent with the formation of three-membered rings. Network modification should favor smaller membered rings upon decompression as the ^{III}O species revert back to bridging oxygens while still compacted.

The Raman spectrum of the sample quenched from 56 GPa is compared to the ambient g-GeO_2 spectrum in Fig. 6. The quenched spectrum indicates some permanent

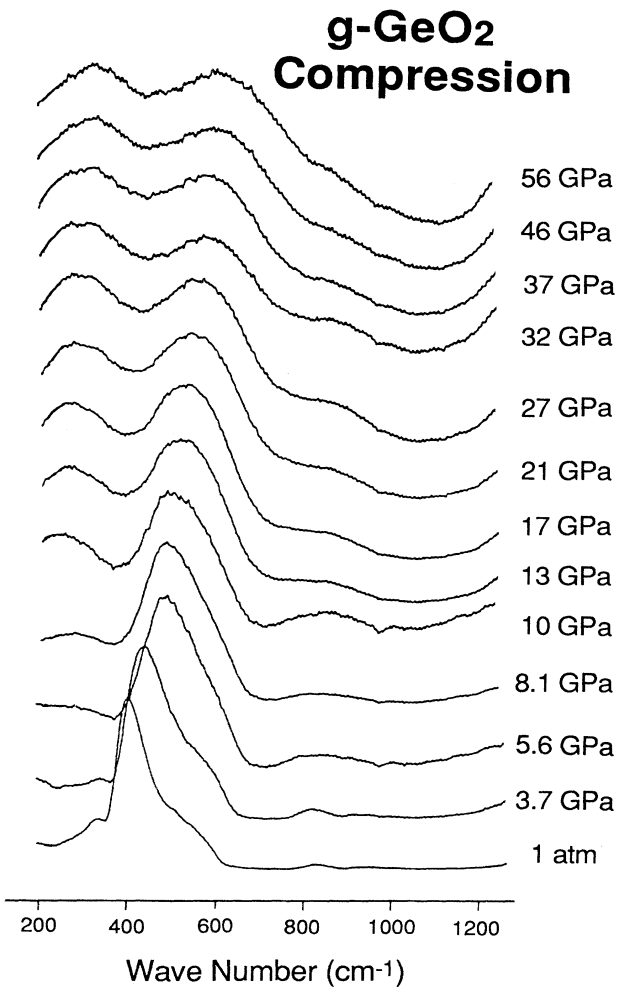

FIG. 3. Composite plot of the *in situ* polarized Raman spectra of GeO_2 glass as a function of pressure from ambient pressure to approximately 56 GPa.

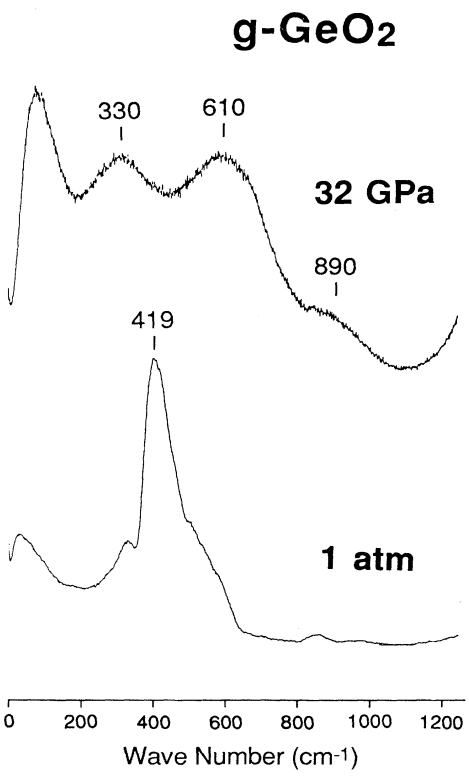

FIG. 4. Comparison of the *HH* Raman spectra of GeO_2 glass at ambient pressure and 32 GPa collected in single-channel scanning mode.

pressure-induced structural changes consistent with previous studies showing a permanent densification in the glass upon decompression from high pressure.[14,18,20,21,83] Both the main Raman band and the high-frequency bands have retained some of their high-pressure frequency shifts, an indication that the glass has not fully relaxed to its initial ambient state. The tetrahedra may retain some of their higher density pressure-induced distortion, while the enhanced 520-cm^{-1} band is consistent with an increase in the population of higher density three-membered rings. Raman spectra of pressure quenched SiO_2 (Ref. 24) and sodium tetrasilicate[25] glasses show similar residual frequency shifts and defect band enhancement.

IV. SUMMARY

In the Raman data of g-GeO_2 under initial compression to 5.6 GPa, the main 419-cm^{-1} Raman band displays a positive frequency shift and broadens with a gradual loss of intensity, consistent with increasing distortion of GeO_4 tetrahedra accompanied by a small decrease in the average intertetrahedral angle. This is in contrast to g-SiO_2 in which the decrease in intertetrahedral angles dominates the initial compression mechanism, with little tetrahedral distortion.[19,20,24,26,81] However, the Raman spectra of g-SiO_2 from 8 to 30 GPa (Ref. 24) qualitatively parallel the Raman spectra of g-GeO_2 under initial compression, suggesting similar compression mechanisms for g-GeO_2 and g-SiO_2 in these pressure ranges.

In accord with a recent EXAFS study,[30] a pressure-induced fourfold to sixfold Ge coordination change in g-GeO_2 is inferred by the Raman spectra between 5.6 and 13 GPa. The coordination change is marked by a change in the pressure derivative of the frequency shift of the main Raman band. This is accompanied by a broadening, and a large intensity decrease in this band, and by the gradual appearance of a new broadband near 240 cm^{-1}. The spectral changes are consistent with a cation coordination change that occurs through the formation of ^{III}O species with no bond breaking. Similar trends observed in the Raman spectra of SiO_2 (Ref. 24) and sodium tetrasilicate[25] glasses at much higher pressures may indicate a similar coordination change.

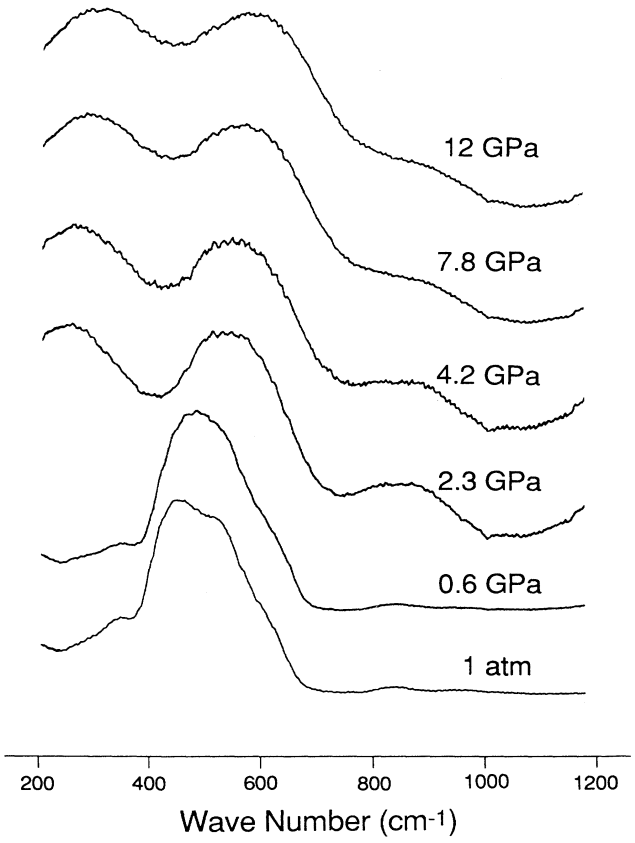

FIG. 5. *In situ HH* Raman spectra of GeO_2 glass under decompression.

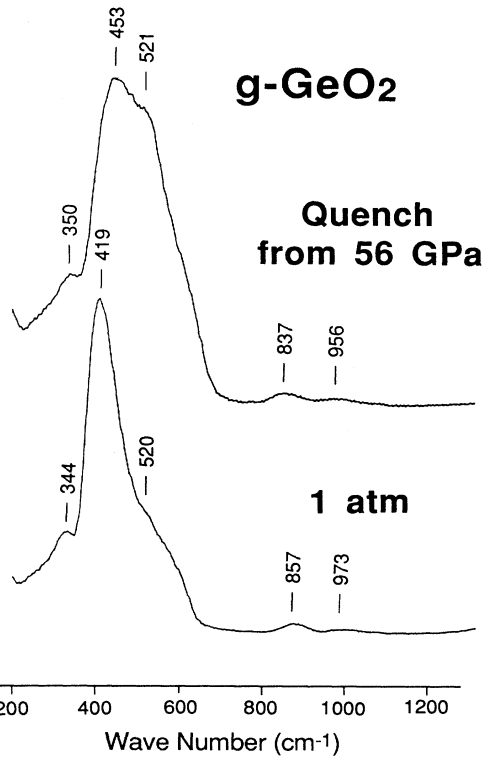

FIG. 6. Comparison of *HH* Raman spectra of GeO_2 glass quenched from 56 GPa with that of the normal unpressurized glass.

After the coordination change is complete by 13 GPa, no further dramatic structural changes are inferred from the Raman spectra up to 56 GPa. Three weak, broad-bands are retained at very high pressures and continue to gradually broaden and shift to higher frequency.

Upon decompression, the Raman spectra indicate that the high-coordinate g-GeO_2 structure is hysteretically retained to at least 2.3 GPa but, significantly, is not quenched to ambient pressure. While the coordination change is fully reversible, some permanent structural modifications in the quenched sample are evident from the Raman spectrum, consistent with a permanent densification of the glass. This includes an increase in the population of defects represented by the 520-cm^{-1} defect band. This is consistent with an increase in the population of high-density three-membered rings as a result of the reversion of ^{III}O species to bridging ^{II}O species upon decompression. Similar trends are observed in the Raman spectra of SiO_2 (Ref. 24) and sodium tetrasilicate[25] glasses decompressed from high pressures.

These observations emphasize the utility of g-GeO_2 as a model for pressure-induced structural changes in tetrahedral oxide glasses and stress the importance of *in situ* studies to the understanding of these high-pressure structures.

ACKNOWLEDGMENTS

The authors thank P. McMillan and A. Angell for many useful and inspired discussions on glass structure. This work was supported by the National Science Foundation under Grant No. EAR-8657437 and by the Shell Graduate Grants Program. The Raman instrument was purchased with funds from Arizona State University and National Science Foundation Grant No. EAR-8709344.

[1]R. Bruckner, J. Non-Cryst. Solids **5**, 123 (1970).
[2]P. Richet, Geochim. Cosmochim. Acta **48**, 471 (1984).
[3]Y. Bottinga and D. F. Weill, Am. J. Sci. **272**, 438 (1972).
[4]H. Verweij and J. H. J. M. Buster, J. Non-Cryst. Solids **34**, 81 (1979).
[5]T. Furakawa and W. B. White, J. Mater. Sci. **15**, 1648 (1980).
[6]M. Ueno, M. Misawa, and K. Suzuki, Physica B **120**, 347 (1983).
[7]C. D. Yin, H. Morikawa, F. Marumo, Y. Gohshi, Y. Z. Bai, and S. Fukushima, J. Non-Cryst. Solids **69**, 97 (1984).
[8]K. Kamiya, T. Yoko, Y. Itoh, and S. Sakka, J. Non-Cryst. Solids **79**, 285 (1986).
[9]K. Kamiya, T. Yoko, Y. Miki, Y. Itoh and S. Sakka, J. Non-Cryst. Solids **91**, 279 (1987).
[10]K. Kamiya, T. Yoko, Y. Miki, and S. Sakka, J. Non-Cryst. Solids **95**, 209 (1987).
[11]P. W. Bridgman, Proc. Am. Acad. Arts Sci. **76**, 55 (1948).
[12]C. Meade and R. Jeanolz, Phys. Rev. B **35**, 236 (1987).
[13]F. Birch and R. B. Dow, Bull. Geol. Soc. Am. **47**, 1235 (1936).
[14]S. K. Sharma, D. Virgo, and I. Kushiro, J. Non-Cryst. Solids **33**, 235 (1979).
[15]C. A. Angell, P. A. Cheesman, and S. T. Tamaddon, Science **218**, 885 (1982).
[16]C. A. Angell, P. A. Cheesman, and S. Tamaddon, Bull. Mineral. **106**, 87 (1983).
[17]P. W. Bridgman, and I. Simon, J. Appl. Phys. **24**, 405 (1953).
[18]H. M. Cohen and R. Roy, J. Am. Ceram. Soc. **44**, 523 (1961).
[19]J. D. Mackenzie, J. Am. Ceram. Soc. **46**, 461 (1963).
[20]H. M. Cohen and R. Roy, Phys. Chem. Glasses **6**, 149 (1965).
[21]I. Kushiro, S. K. Sharma, and D. W. Matson, J. Non-Cryst. Solids **71**, 429 (1985).
[22]L. Liu and W. A. Bassett, *Elements, Oxides, and Silicates: High-Pressure Phases with Implications for the Earth's Interior* (Oxford University, New York, 1986).
[23]Q. Williams and R. Jeanloz, Science **239**, 902 (1988).
[24]R. J. Hemley, H. K. Mao, P. M. Bell, and B. O. Mysen, Phys. Rev. Lett. **57**, 747 (1986).
[25]G. H. Wolf, D. J. Durben, and P. F. McMillan, J. Chem. Phys. **93**, 2280 (1990).
[26]F. A. Seifert, B. O. Mysen, and D. Virgo, Geochim. Cosmochim. Acta **45**, 1879 (1981).
[27]A. E. Ringwood, *Composition and Petrology of the Earth's Mantle* (McGraw-Hill, New York, 1975), p. 356.
[28]J. F. Scott, Phys. Rev. B **1**, 3488 (1970).
[29]I. Jackson, Phys. Earth Planet. Inter. **13**, 218 (1976).
[30]J. P. Itie, A. Polian, G. Calas, J. Petiau, A. Fontaine, and H. Tolentino, Phys. Rev. Lett. **63**, 398 (1989).
[31]H. K. Mao, P. M. Bell, K. J. Dunn, R. M. Chrenko, and R. C. Devries, Rev. Sci. Instrum. **50**, 1002 (1979).
[32]A. P. Jephcoat, H. K. Mao, and P. M. Bell, in *Hydrothermal Experimental Techniques,* edited by G. C. Ulmer and H. L. Barnes (Wiley-Interscience, New York, 1987), p. 469.
[33]H. K. Mao, P. M. Bell, J. W. Shanner, and D. J. Steinberg, J. Appl. Phys. **49**, 3276 (1978).
[34]J. F. Mammone and S. K. Sharma, Carnegie Inst. Wash. Year Book **78**, 640 (1978).
[35]A. J. Leadbetter and A. C. Wright, J. Non-Cryst. Solids **7**, 37 (1972).
[36]P. Bondot, Phys. Status Solidi A **22**, 511 (1974).
[37]K. Tanaka, Philos. Mag. Lett. **57**, 183 (1988).
[38]E. Lorch, J. Phys. C **2**, 229 (1969).
[39]G. A. Ferguson and M. Hass, J. Am. Ceram. Soc. **53**, 109 (1970).
[40]J. A. E. Desa and A. C. Wright, J. Non-Cryst. Solids **99**, 276 (1988).
[41]L. Cervinka, J. Non-Cryst. Solids **106**, 291 (1988).
[42]D. E. Sayers, E. A. Stern, and F. W. Lytle, Phys. Rev. Lett. **35**, 584 (1975).
[43]M. Okuno, C. D. Yin, H. Morikawa, and F. Marumo, J. Non-Cryst. Solids **87**, 312 (1986).
[44]F. L. Galeener and G. Lucovsky, Phys. Rev. Lett. **37**, 1474 (1976).
[45]F. L. Galeener, J. Non-Cryst. Solids **40**, 527 (1980).
[46]F. L. Galeener, A. J. Leadbetter, and M. W. Stringfellow, Phys. Rev. B **27**, 1052 (1983).
[47]F. L. Galeener, A. E. Geissberger, G. W. Ogar, Jr., and R. E. Loehman, Phys. Rev. B **28**, 4768 (1983).
[48]S. K. Sharma, D. W. Matson, J. A. Philpotts, and T. L. Roush, J. Non-Cryst. Solids **68**, 99 (1984).
[49]R. L. Mozzi and B. E. Warren, J. Appl. Crystallogr. **2**, 164 (1969).
[50]J. D. Jorgensen, J. Appl. Phys. **49**, 5473 (1978).
[51]W. H. Zachariasen, J. Am. Chem. Soc. **54**, 3841 (1932).
[52]C. Glidewell, Inorg. Chim. Acta **12**, 219 (1975).

[53]M. O'Keeffe and B. G. Hyde, Acta Crystallogr. B **34**, 27 (1978).
[54]M. O'Keeffe and B. G. Hyde, in *Structure and Bonding in Crystals,* edited by M. O'Keeffe and A. Navrotsky (Academic, New York, 1981), Vol. 1, p. 227.
[55]J. C. Phillips, Phys. Today **35**(2), 27 (1982).
[56]J. C. Phillips, Solid State Phys. **37**, 93 (1982).
[57]J. R. Banavar and J. C. Phillips, Phys. Rev. B **28**, 4716 (1983).
[58]J. C. Phillips, J. Non-Cryst. Solids **63**, 347 (1984).
[59]J. C. Phillips, Solid State Commun. **60**, 299 (1986).
[60]J. L. Galeener, Solid State Commun. **44**, 1037 (1982).
[61]J. L. Galeener, J. Non-Cryst. Solids **49**, 53 (1982).
[62]J. L. Galeener, in *Physics of Disordered Materials,* edited by D. Adler, H. Fritzsche, and S. R. Ovshinsky (Plenum, New York, 1985), p. 159.
[63]B. Bridge, N. D. Patel, and D. N. Waters, Phys. Status Solidi **77**, 655 (1983).
[64]H. Verweij, J. Non-Cryst. Solids **33**, 41 (1979).
[65]H. Verweij, J. Non-Cryst. Solids **33**, 55 (1979).
[66]G. S. Henderson, G. M. Bancroft, and M. E. Fleet, Am. Mineral. **70**, 946 (1985).
[67]F. L. Galeener and R. H. Geils, in *The Structure of Non-Crystalline Materials,* edited by P. H. Gaskell (Taylor and Francis, London, 1977), p. 223.
[68]R. J. Bell, N. F. Bird, and P. Dean, J. Phys. C **1**, 299 (1968).
[69]R. J. Bell, P. Dean and D. C. Hibbins-Butler, J. Phys. C **3**, 2111 (1970).
[70]R. J. Bell and D. C. Hibbins-Butler, J. Phys. C **8**, 787 (1975).
[71]P. N. Sen and M. F. Thorpe, Phys. Rev. B **15**, 4030 (1977).
[72]R. B. Laughlin and J. D. Joannopoulos, Phys. Rev. B **16**, 2942 (1977).
[73]R. B. Laughlin and J. D. Joannopoulos, Phys. Rev. B **17**, 2790 (1978).
[74]R. B. Laughlin and J. D. Joannopoulos, Phys. Rev. B **17**, 4922 (1978).
[75]F. L. Galeener, Phys. Rev. B **19**, 4292 (1979).
[76]R. A. Barrio, F. L. Galeener, and E. Martinez, Phys. Rev. B **31**, 7779 (1985).
[77]F. L. Galeener, R. A. Barrio, E. Martinez, and R. J. Elliott, Phys. Rev. Lett. **53**, 2429 (1984).
[78]M. E. Fleet, C. T. Herzberg, G. S. Henderson, E. D Crozier, M. D. Osborne, and C. M. Scarfe, Geochim. Cosmochim. Acta **48**, 1455 (1984).
[79]B. Houser, N. Alberding, R. Ingalls, E. D. Crozier, Phys. Rev. B **37**, 6513 (1988).
[80]F. L. Galeener, in *Excitations in Disordered Systems,* edited by M. F. Thorpe (Plenum, New York, 1982), p. 359.
[81]R. A. B. Devine, R. Dupree, I. Farnan, and J. J. Capponi, Phys. Rev. B **15**, 2560 (1987).
[82]J. G. Traylor, H. G. Smith, R. M. Nicklow, and M. K. Wilkinson, Phys. Rev. B **3**, 3457 (1971).
[83]M. Grimsditch, R. Bhadra, and Y. Meng, Phys. Rev. B **38**, 7836 (1988).